Egyptian Journal of Petroleum (2015) 24, 255–263

HOSTED BY

Egyptian Petroleum Research Institute

Egyptian Journal of Petroleum

www.elsevier.com/locate/egyjp
www.sciencedirect.com

FULL LENGTH ARTICLE

Groundwater exploration using resistivity and magnetic data at the northwestern part of the Gulf of Suez, Egypt

Abdel Galil A. Hewaidy [a], Essam A. El-Motaal [a], Sultan A. Sultan [b], Talaat M. Ramdan [c], Ahmed A. El khafif [d], Shokry A. Soliman [d,*]

[a] *Faculty of Science Al-Azhar University, Egypt*
[b] *National Research Institute of Astronomy and Geophysics, Egypt*
[c] *National Authority of Remote Sensing, Egypt*
[d] *Egyptian Petroleum Research Institute, Egypt*

Received 26 March 2014; accepted 21 May 2014
Available online 23 July 2015

KEYWORDS

Schlumberger configuration;
Groundwater aquifer;
Structures;
Magnetic

Abstract The present study aims to investigate the ground water accumulations present in the area located west of the Gulf of Suez, to face the new urbanization settlements of industrial national projects in the study area using geoelectrical and magnetic measurements. Magnetic data interpretation was carried out using the RTP magnetic data (or, through analyzing the RTP aeromagnetic map) to determine the depth to the surface of basement rocks and delineate the trends of structural elements. The results of magnetic interpretation indicated that the depth to the basement surface is ranging from 1200 to 3500 m and the trends of encountered structural elements are mainly NE–SW, NW–SE, NNW–SSE and E–W directions. Seventeen vertical electrical soundings of Schlumberger configuration were measured with AB/2 ranging from 1.5 m to 1500 m at the southern part of the study area. The results of quantitative interpretation of geoelectrical data indicated that the subsurface section consists of six different geoelectrical units; the first unit represents the Quaternary gravel and sand of high resistivity values and thickness of about a few meters. The second geoelectrical unit exhibits moderate resistivity values ranging from 23 to 100 ohm m and thickness ranging from 4.5 to 67 m which represents the fresh water aquifer in the study area, while the lithology of this layer consists of sandstone and limestone which belongs to the Upper Miocene. The third geoelectrical unit is composed of sandy clay and limestone which belongs to the Middle Miocene deposits and shows low resistivity values ranging from 6 to 7 ohm m and thickness ranging from 44.5 m to 66 m. This third layer represents the second aquifer (brackish water). The fourth geoelectrical unit consists of limestone and clayey limestone which belongs to the Lower Miocene deposits and exhibits moderate resistivity values ranging from 16 to 33 ohm m, while the thickness of this unit ranges from 47–102 m. This layer represents the third aquifer (brackish water). The fifth geoelectrical unit reveals very low resistivity values of about 2–5 ohm m and

* Corresponding author.
Peer review under responsibility of Egyptian Petroleum Research Institute.

http://dx.doi.org/10.1016/j.ejpe.2015.07.010

consists of clay and sandstone of the Oligocene and Upper Eocene deposits. The sixth geoelectrical unit is the bottommost unit in the studied subsurface section and exhibits moderate resistivity values in a range of about 22–35 ohm m and consists of limestone of the Middle Eocene deposits.

1. Introduction

Different authors used different geophysical tools such as resistivity and magnetism for ground water exploration [1–3]. [1] studied the ground water potentiality at the southern part of the study area; and they concluded that; the ground water in this area is accumulated in the Upper Miocene, Middle Miocene and Lower Miocene deposits. The study area is located between latitudes 29° 30′ to 30° 00′ N and longitudes 32° 00′ & 32° 30′ E (Fig. 1).

The western side of the Gulf of Suez is one of the proposed promising sites for new urbanization programs of industrial national projects. The present study aims to investigate the ground water occurrences to face the increasing new water demands of the industrial national projects as the cement, fertilizers, ceramics and steel factories in the study area, using geoelectrical measurements.

1.1. Geology of the study area

In the study area, different rock units were identified. They range in age from the Jurassic to Quaternary. Eocene, Oligocene and Miocene are the most widespread rock units in this area (Fig. 2) according to [4]. The Jurassic section consists of varicolored and cross-bedded sandstones, with mudstone and siltstone interbeds. The Cretaceous succession in the study area is classified by [5] into three rock units, which are (from base to top) the Malha, Galala and chalky limestone units. The Eocene rocks are the nummulitic limestones, which form the main part of Gabal Ataqa and Gabal El-Galala El-Baharyia as well as the faulted blocks of Akheider-Rammlyia and Um Zeita-Kahallya. The Eocene succession is subdivided from base to top into the upper part of Esna Shale Formation, Farafra Formation, Thebes Formation, Muweilih Formation, Mokattam Formation, Observatory Formation, Qurn Formation, Wadi Garawi Formation and Wadi Hof Formation. The Oligocene rocks are differentiated into two units; the lower unit is varicolored, consisting of unstratified sands, gravels, and sedimentary quartzites; the upper unit crops out in the central part of the study area and consists of basalt sheets of Gabal El Ahmer Formation. The Miocene succession that is exposed in the Sadat area lies 30 km to the southwest of Suez city and is subdivided from base to top as follows: Sadat Formation (Early Miocene), Hommath Formation (Middle Miocene) and Hagul Formation (Late Miocene). Sands, gravels, clays, sabkhas and sand accumulations represent the recent deposits in the study area.

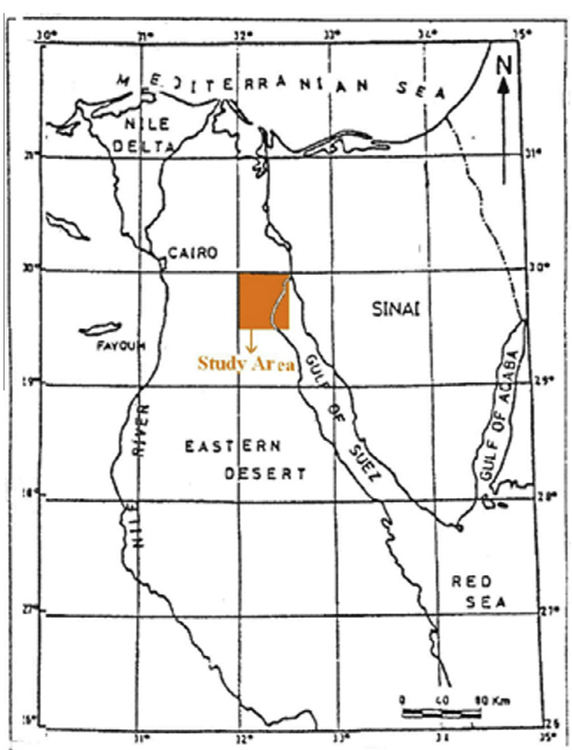

Figure 1 Location map of the study area.

2. Methodology

2.1. Magnetic data and interpretation

2.1.1. Acquisition and enhancement of magnetic data

The airborne geophysical magnetic surveys for the study area were carried out by [6]. The obtained airborne magnetic data were reduced to the north magnetic pole (RTP), compiled and finally presented in the form of RTP aeromagnetic map reduced to the pole (Fig. 3). The map reveals a high magnetic anomaly occupying the northeastern, northwestern and eastern parts of the study area, while the low magnetic anomaly occupys the southwestern part.

2.1.2. Interpretation of magnetic data

2.1.2.1. Magnetic filtering. The high and low pass filter technique based on wave number was applied on the RTP aeromagnetic map reduced to the pole data (Fig. 3) to separate the residual and regional magnetic anomalies. The separation was carried out at a wave number cut-off of 0.0000287 (1/km) through the power spectrum technique (Fig. 4), RTP aeromagnetic producing two maps representing the residual (Fig. 5) and regional magnetic anomaly maps using [7]. The qualitative interpretation of the RTP map shows that, the zones of high gradient with closely spaced contour lines are indicators of probable major fault zones. Also, the direction

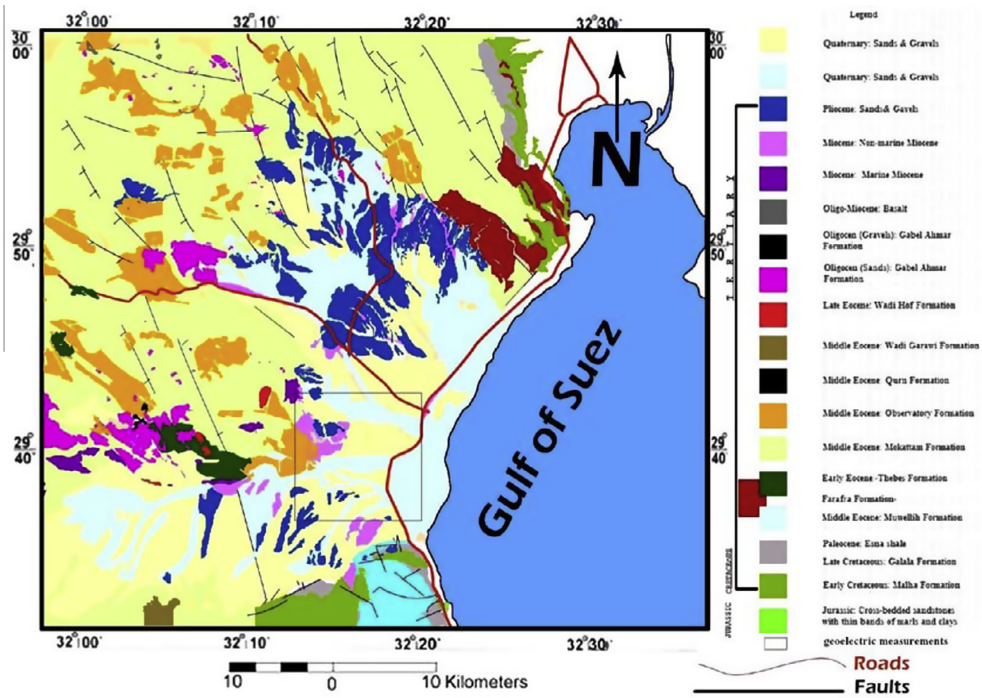

Figure 2 Geologic map of the study area after [4] and geoelectric measurement.

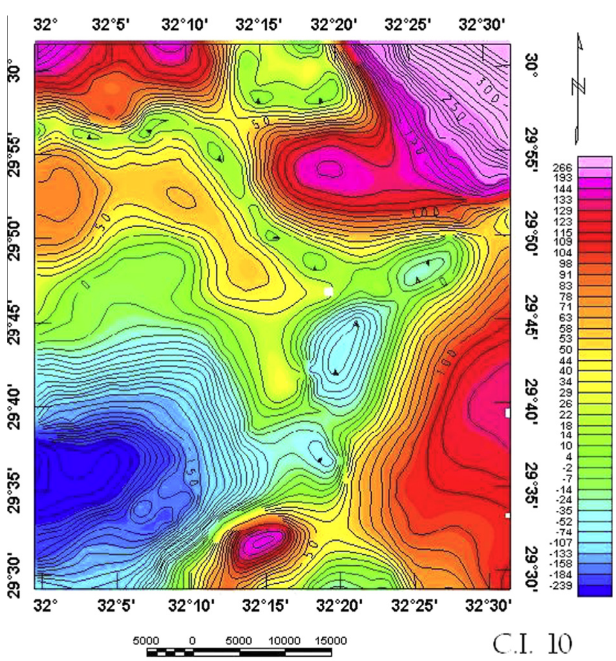

Figure 3 The RTP aeromagnetic map.

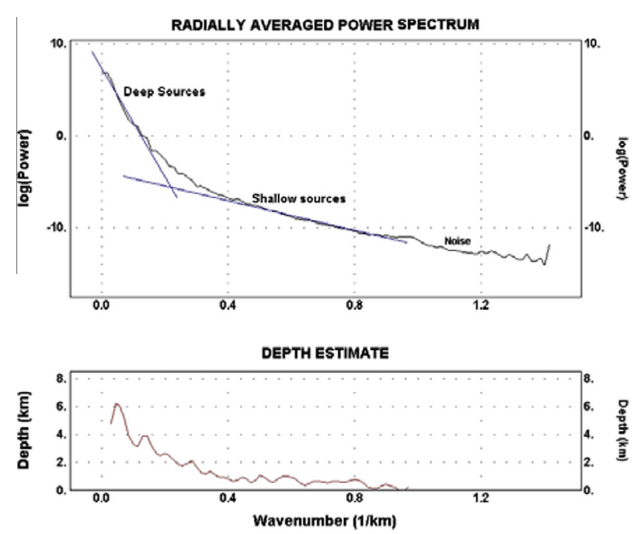

Figure 4 Power spectrum showing the mean depth to the basement rock in the area.

of the downthrown side of faults is taken as the direction of decreasing values of the contours. By this way, the fault elements were determined as shown in (Fig. 6). The predominant trends of faults include four sets, oriented in N–E, N–W, NNW and E–W directions. Besides, the minor fault trends are also encountered.

2.1.2.2. Magnetic modeling. The magnetic modeling was carried out through five magnetic profiles (Fig. 7) crossing the magnetic anomalies and trending East–West. Through the use of [8] and using the measured magnetic susceptibility of 0.00229 cgs units for the basement rocks, it was possible to delineate the shape of the basement surface and the overlying sedimentary cover, where the depths to the surface of basement rocks are varying along the different locations of the study area, as shown in (Fig. 8).

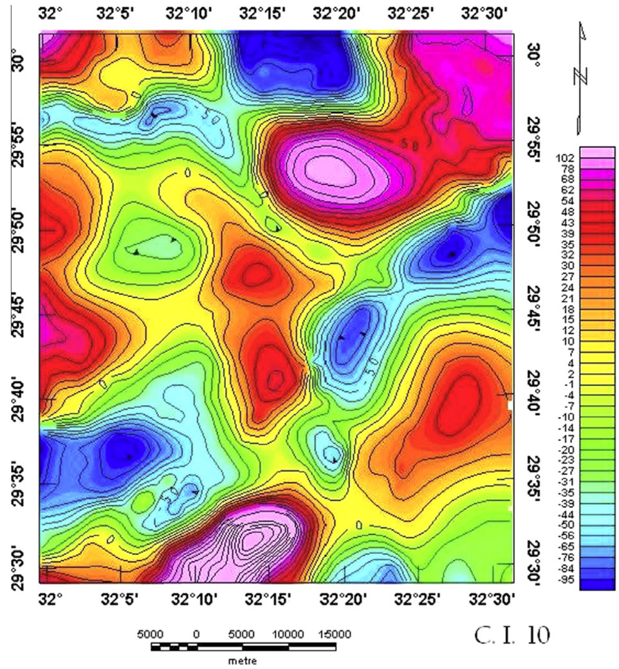

Figure 5 Residual aeromagnetic map.

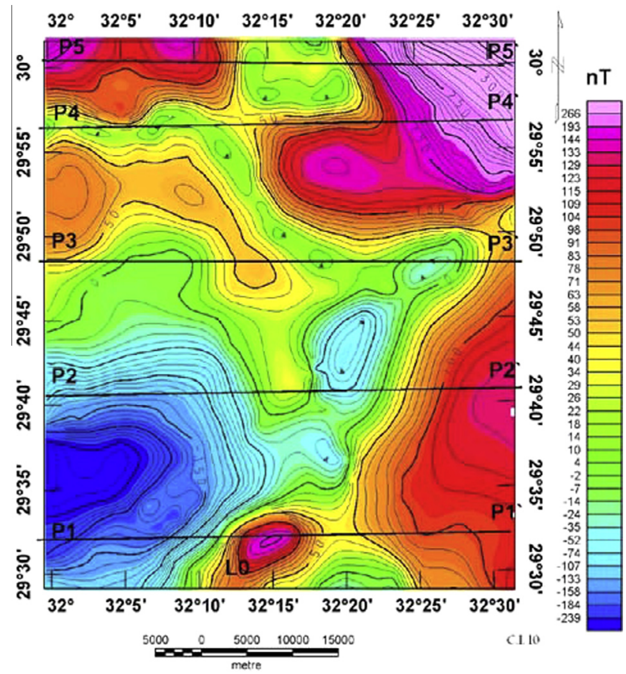

Figure 7 Location of the magnetic profiles used for 2D modeling.

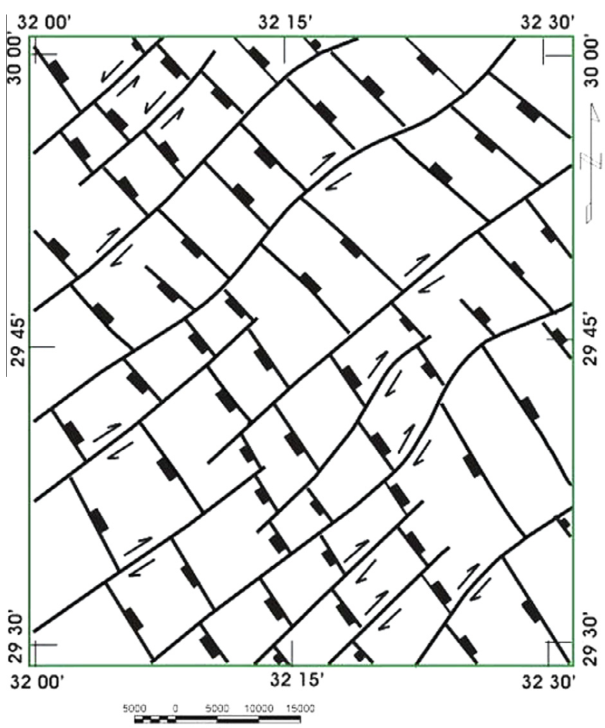

Figure 6 Fault elements dissecting the study area.

2.1.2.3. Magnetic depth. The quantitative interpretation of the magnetic basement depths indicated that, the depth of the basement surface is deeper at the southern part, where the depth reaches about 3500 m. Also, the depth of the basement surface is deep at the northwestern part, where the depth reaches about 3200 m. The central part of the study area is occupied by shallow depths of the basement surface of about 1200 m (Fig. 9).

2.2. Geoelectrical data interpretation

2.2.1. Field work and geoelectrical acquisition

The vertical electrical sounding (VES) measurements were carried out by using a Russian electronic compensator, type AE-72. The resistivity measurements were recorded twice, after changing the supply voltage. The mean relative measuring error reached about 2%. By this way, seventeen vertical electrical soundings were measured in the area under investigation (Fig. 10). The well known Schlumberger configuration (VES) of electrode separation ranging from AB/2 = 1.5 m to AB/2 = 1500 m was used for measuring the seventeen VES stations.

2.2.2. Quantitative interpretation

The aim of quantitative interpretation of the vertical electrical soundings is to determine the thicknesses and true resistivity values of the successive strata below the different stations, utilizing the measured field data, which are represented by plotting the apparent resistivity values against AB/2 spacing. There are several methods for the quantitative interpretation of electrical data. Few of them are graphical and the major sophisticated ones are the analytical methods, which, recently, depend on using computer softwares. In the present study, the analytical method was carried out using the (computer program), which is defined by [9]. First, the surveyed resistivity data were analyzed manually, and the obtained results of the manual interpretation were used as initial models for the analytical methods required for the computer software. This program deals with the VES curves in a man-computer

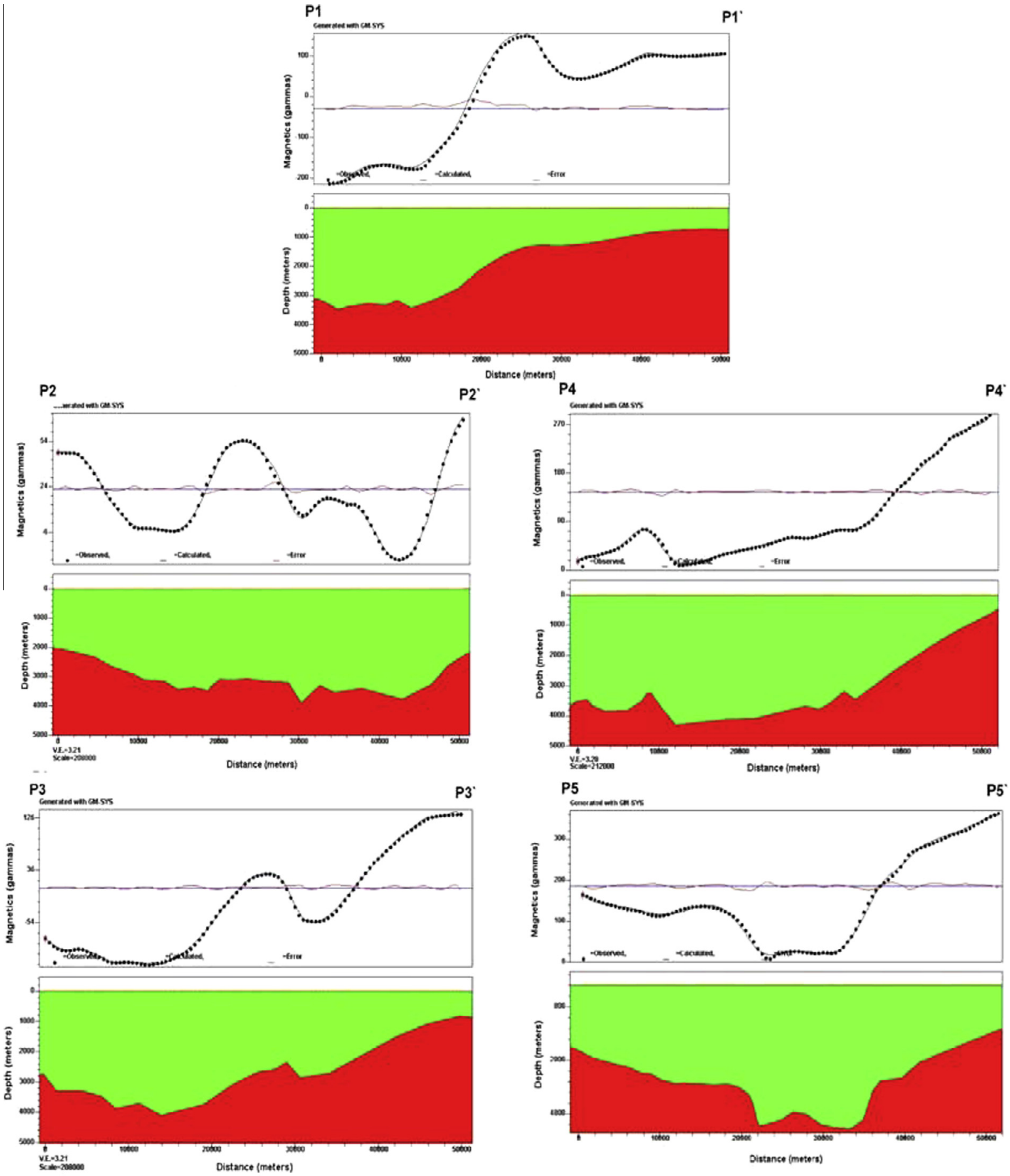

Figure 8 2 D Magnetic Modeling along profiles P1–P1′, P2–P2′, P3–P3′, P4–P4′ and P5–P5′.

interactive regime and draws the theoretical and field curves on a display screen together with the Rho (z) model curve. The quantitative interpretation has been applied to determine the thicknesses and true resistivities of the lithological units below each VES station. The final results were used for the construction of geoelectrical cross-sections which exhibit the different geological units existing in the study area.

2.2.3. Geoelectrical cross sections

The geoelectrical cross-sections A–A′, B–B′, C–C and D–D. (Figs. 11–14) reveal six geoelectrical units. The first unit represents Quaternary gravel and sand of high resistivity values and thickness of about a few meters. The second geoelectrical unit exhibits resistivity values ranging from 23 to 100 ohm m and represents the fresh water aquifer in the study area, while the thickness ranged from 4.5 m at VES station 1 to 67 m at VES

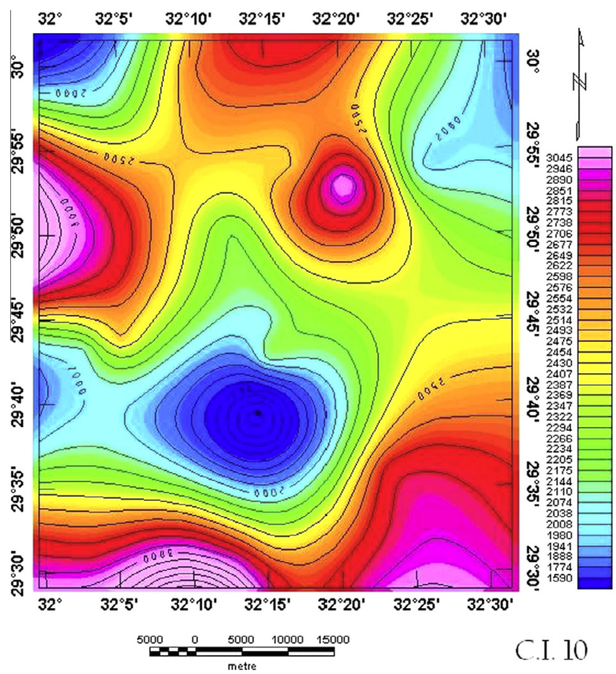

Figure 9 Magnetic depth map of the study area.

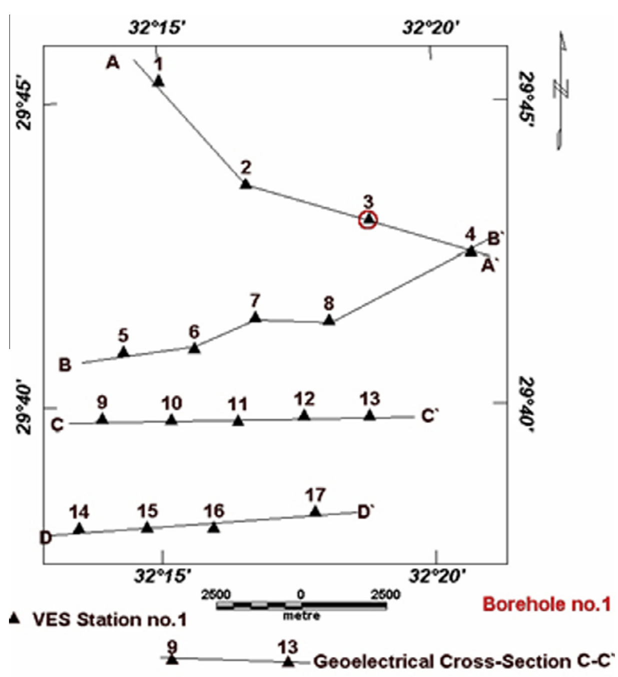

Figure 10 Location map showing the VES stations and directions of studied resistivity profiles within the study area.

station 3, the lithology of this layer consists of sandstone and limestone which belongs to the Upper Miocene. The third geoelectrical unit is composed of sandy clay and limestone which belongs to the Middle Miocene deposits and have resistivity values ranging from 6 to 7 ohm m and thickness that ranged from 44.5 to 66 m. This layer represents the second aquifer (of brackish water). The fourth geoelectrical cross-section represents a unit which consists of limestone and clayey limestone that belongs to the Lower Miocene deposits and exhibit moderate resistivity values ranging from 16 ohm m to 33 ohm m. The thickness of this unit ranges from 47 m at VES station 12 to 102 m at VES station 17. This layer represents the third aquifer (brackish water). The fifth geoelectrical unit reveals very low resistivity values of 2–5 ohm m and consists of clay and sandstone of the Oligocene and Upper Eocene deposits. The thickness ranges from 40 to 113 m. The sixth geoelectrical unit is the bottommost unit in the studied section and its upper surface was detected only at VES stations 1 and 3 and exhibits moderate resistivity values that range from 22 ohm m to 35 ohm m and consists of limestone of the Middle Eocene deposits.

2.2.4. Isoresistivity map of the second geoelectrical unit

The resistivity values range from 10 ohm to 600 ohm, in which the maximum resistivity is represented at the southern part, while the minimum resistivity is exhibited within most of the northern part of the study area (Fig. 15).

2.2.5. Isopach map of the second geoelectrical unit

The isopach map of this unit exhibits considerable thickness at the northern and northeastern part with a thickness that reaches 85 m, while the northwestern part is characterized by small thickness of about 5 m. This layer represents the fresh water aquifer in the study area. The lithology of this layer consists of limestone and sandstone (Fig 16).

2.2.6. Depth map of the second geoelectrical unit

The depth to the top of the second geoelectrical unit is represented by Fig. 17 which shows shallow depths at the northwestern and the southeastern parts of the study area (1–5 m), but the northeastern and southwestern parts reveal deeper depths (20–25 m).

3. Discussion

The results obtained from the interpretation of the geoelectrical data of vertical electrical sounding number 3, indicate that; the thickness of the first unit reaches a few meters, the second geoelectrical unit represents the fresh water aquifer in the study area with a thickness of about 67 m, the third geoelectrical unit has a thickness of about 44.5 m, the fourth geoelectrical unit with a thickness of about 102 m and the fifth geoelectrical unit with a thickness of about 113 m. Generally, the results of the interpretations of the geoelectrical data are compatible with the results obtained from the bore holes number 1 drilled by EGSMA 1999. The VES No. 3 where the second layer indicates that the thickness of about 67 m is correlated with the true thickness derived from the drilled well-1 and that is confirming our results.

4. Conclusion

According to the results of the interpretation of the aeromagnetic and geoelectric data, in the present study, it can be concluded that:

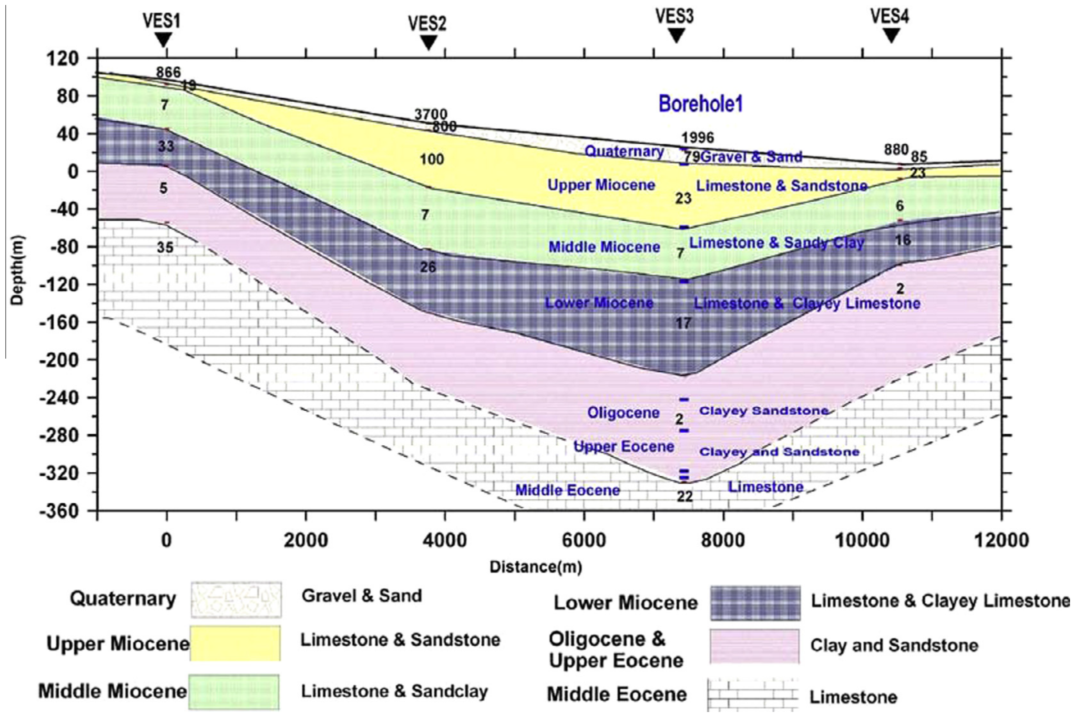

Figure 11 Geoelectrical cross-section along profile A–A′.

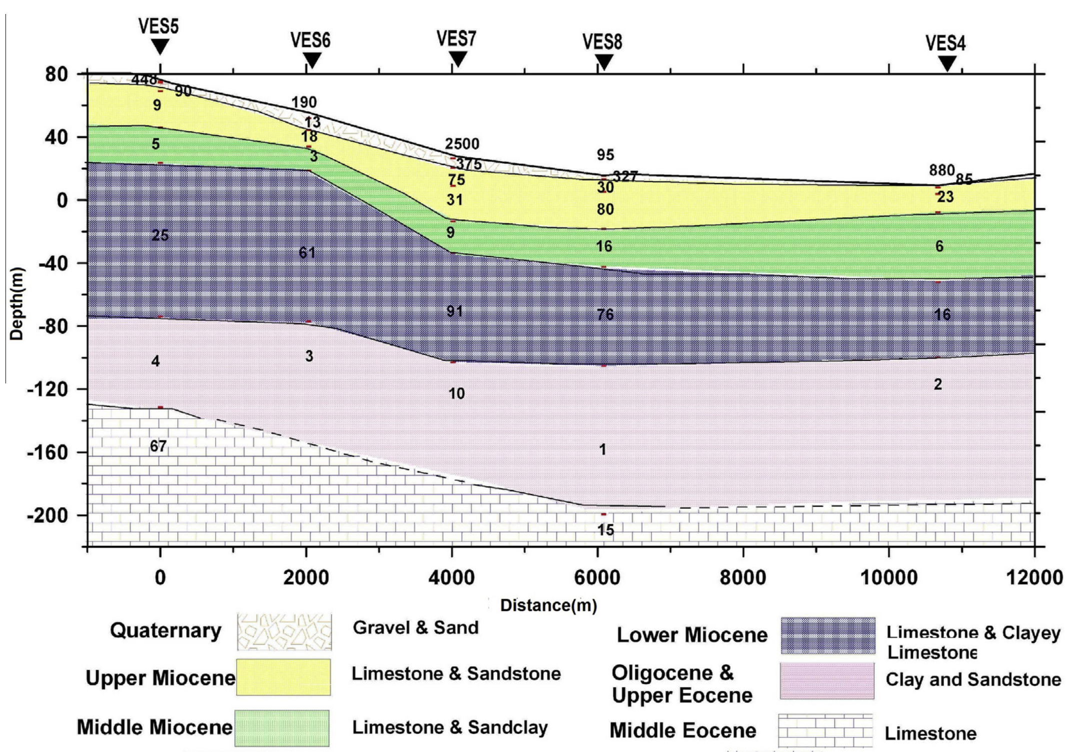

Figure 12 Geoelectrical cross-section along profile B–B′.

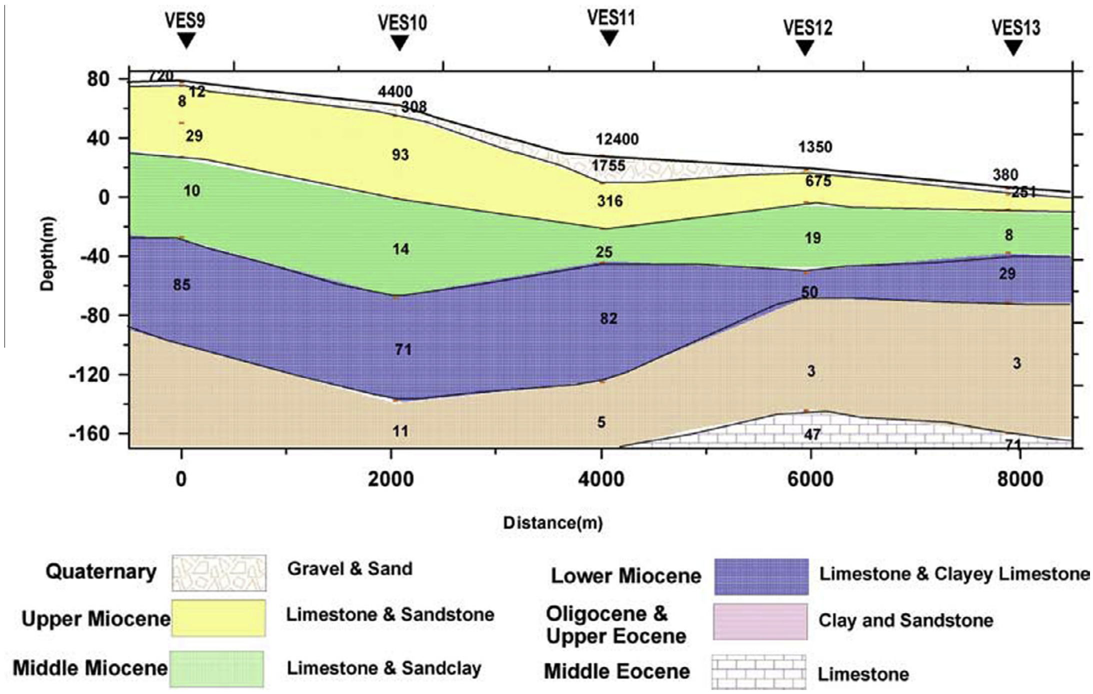

Figure 13 Geoelectrical cross-section along profile C–C′.

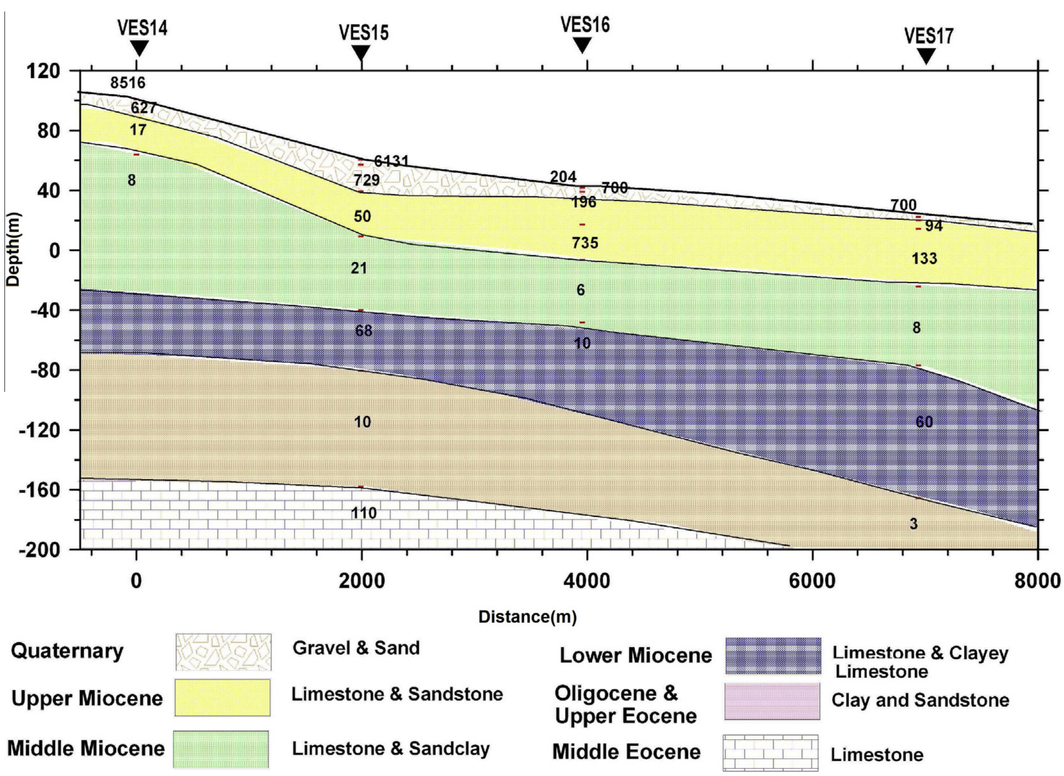

Figure 14 Geoelectrical cross-section along profile D–D′.

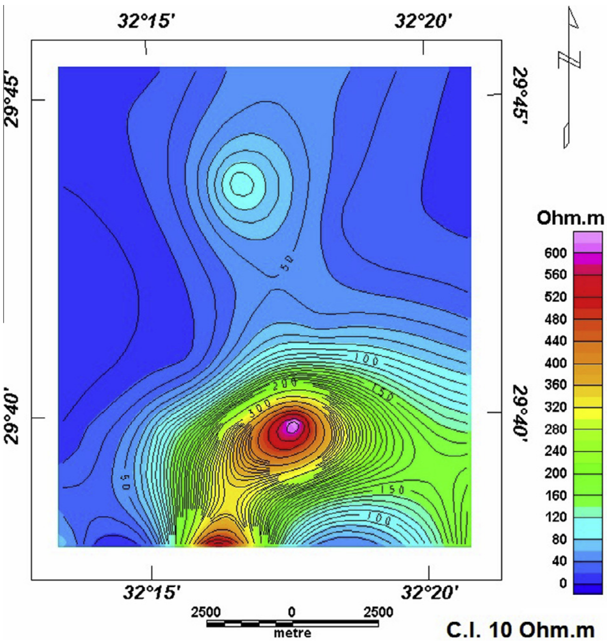

Figure 15 Iso-resistivity map for the second geoelectrical unit.

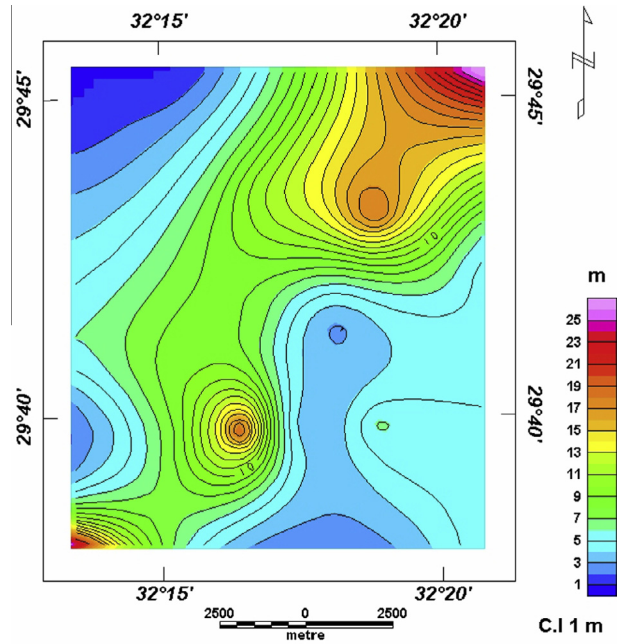

Figure 17 Depth map for the second geoelectrical unit.

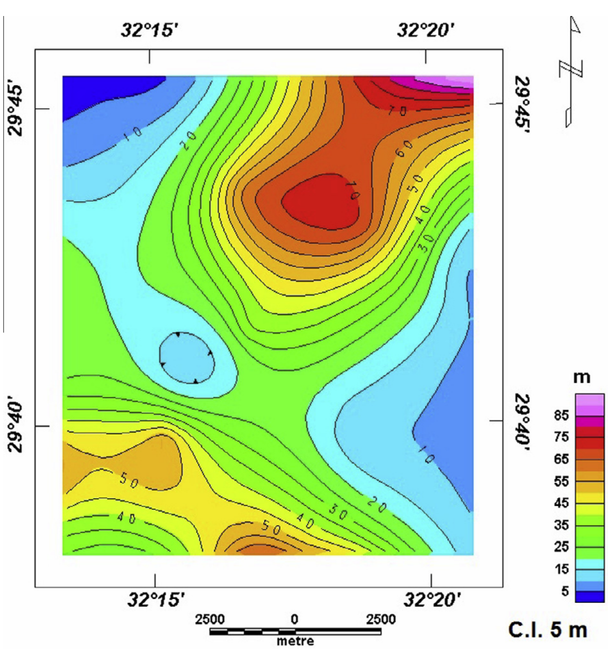

Figure 16 Isopach map for the second geoelectrical unit.

1. The depth of basement surfaces ranges from 1200 to 3500 m and the trends of structural elements in the study area have directions NE–SW, NW–SE, NNW–SSE and E–W.
2. The study area is formed mainly of six different geoelectrical units. These units belong to the Quaternary, Upper Miocene, Middle Miocene, Lower Miocene, Oligocene and Upper Eocene and Middle Eocene deposits.
3. The groundwater in the study area is accumulated in the Upper Miocene, Middle Miocene, and Lower Miocene deposits.
4. The thickness and depth values for different layers encountered in the study area indicated that, the fresh water-bearing aquifer has a thickness ranging from 5 to 85 m and a depth varying from 5 to 25 m from the earth's surface.

References

[1] S.A. Sultan, B.S. Mohamed, Ann. Geol. Surv. Egypt V.XX111 (2000) 901–918.
[2] S.A. Sultan, NRIAG J. Geophys. 6 (1) (2007) 97–115.
[3] S.A. Sultan, Fernando A.M. Santos, Ahmad S. Helaly, Arab. Geosci. J. (2009), http://dx.doi.org/10.1007/s12517-009-0085-6.
[4] S.M. Hassaan, Studying geological structures of Ayn-Sokhna area, north Eastern Desert, Egypt, by optimum utilization of data fusion techniques of some satellite image (Ph.D. thesis), Fac. Sci., Helwan University, 2008, 207p.
[5] M.A. Abdallah, Structural geology of the area between El Galala El-Baharyia and Gabal Akheider (Ph.D. thesis), Fac. Sci., Ain Shams Univ., Cairo, 1993, 199p.
[6] Aero-Service, Final operational report of airborne magnetic, radiation survey in the Eastern Desert, Egypt for the Egyptian General Petroleum Corporation, Aero-Service, Houston, Texas, Six Volumes, 1984.
[7] Geosoft program, "Geosoft mapping and processing system" Geosoft Inc., suit 500, Richmond st. west Toronto, on Canada N5UIV6, 1994.
[8] GM – SYS program, Gravity and Magnetic Modeling, version 3.6, Northwest Geophysical Association, Inc. (NGA), Corvallis, Oregon, U.S.A., 1999, 97339.
[9] IPI2Win Program, "Programs set for ID VES data interpretation, dep. of geophysics" Geological Faculty, Moscow university. Russia, 2001, 119899.